Poly(Propylene)/Poly(Ethylene Terephthalate-co-Isophthalate) Blends and Glass Bead Filled Composites: Microstructure and Thermomechanical Properties

D. Arencón,[1] J. I. Velasco,[1] M. A. Rodríguez-Pérez,[2] J. A. de Saja[2]

[1]*Centre Català del Plàstic, Universitat Politècnica de Catalunya, Terrassa, Spain*
[2]*Departamento de Física de la Materia Condensada, Cristalografía y Mineralogía, Facultad de Ciencias, Universidad de Valladolid, Valladolid, Spain*

Received 18 December 2003; accepted 25 June 2004
DOI 10.1002/app.21146
Published online in Wiley InterScience (www.interscience.wiley.com).

ABSTRACT: Blends of poly(propylene) (PP) and poly(ethylene terephthalate-co-isophthalate) (co-PET) (95/5) with and without compatibilizing agent (maleic anhydride PP), as well as composites of these blends with glass beads (50 wt%) with and without silane coupling agent surface-treatment, were prepared and studied on a basis of the material microstructure and thermomechanical properties. Infrared and Raman spectroscopy, as well as transmission electron microscopy, displayed evidence of MAPP compatibilizing action for the blend. Differential scanning calorimetry showed a remarkable effect of nucleation rate increase exerted by co-PET on the PP crystallization. Moreover, glass beads were found to increase the PP nucleation rate slightly. PP crystallinity hardly varied with the composition. Wide angle X-ray diffraction allowed determination of differences in the orientation of the poly(propylene) b-axis, with more homogeneous orientations in the presence of both co-PET and glass beads. MAPP promoted the PP b-axis orientation. Differences in PP α' relaxation could be analyzed through dynamic-mechanical thermal analysis (DMTA). © 2004 Wiley Periodicals, Inc. J Appl Polym Sci 94: 1841–1852, 2004

Key words: poly(propylene); poly(ethylene terephthalate-co-isophthalate); blends; fillers; composites

INTRODUCTION

The present article deals with the combined effect of filling PP with a non conventional filler (glass beads), as well as with the effect of blending this polymer with co-PET.

Among particulate filled poly(propylene) composites, glass bead-filled composites are easily processed and have small and well-distributed internal stress, high dimensional stability, and good service performance. Most of the investigations with these kind of composites have been mainly focused on aspects related to the particle size and the filler concentration effect.

Regarding the microstructure of glass bead filled PP, this filler displays a moderate effect of nucleating agent for PP crystallinity,[1] increasing slightly the intensity of this effect with the glass bead concentration. Nevertheless, no effect on the global crystallinity degree has been reported. Contradictory results have been published concerning the effect of glass bead on the PP glass transition temperature (T*g*). Stricker[2] did not find differences in T*g* for different glass bead concentrations; however, Liang and Li[3] noticed a slight increase of T*g* with the filler loading in the range of 0–15% by volume. These authors report[4] that the viscous loss component is not affected by the glass beads content.

In general, a higher melt viscosity is expected as the filler loading is increased.[5] It has also been reported[6] that in spite of both physical and rheological dependencies on the glass bead amount, the flow behavior during injection-molding is governed by PP viscoelasticity.[6]

Increasing the glass bead diameter led to a build-up in the composite stiffness,[7] although the tensile strength and the elongation at break[7,8] as well as the fracture toughness[9] diminished. Similarly, in glass bead filled PP composites, increasing the glass bead concentration results in a stiffness increase and in both tensile strength and elongation at break decrease.[5,7,8] Also, Izod impact strength was found to be reduced,[8] and a brittle-ductile transition located at 10% by volume of glass beads has been reported.[10] The main mechanisms acting during the ductile failure of these filled polymers are the particle-matrix debonding, followed by the matrix yielding and the plastic flow of the micro-ligaments.[8,11]

Correspondence to: J.-I. Velasco (jose.ignacio.velasco@upc.es).

Contract grant sponsor: MCYT (Government of Spain); contract grant numbers: MAT-2000–1112, MAT-2000–0084-P4, and DPI-2000–0184-P4.

Among the many factors that influence mechanical properties of filled poly(propylene), interfacial adhesion is one of the most relevant ones. The mechanical behavior is highly dependent on the interfacial shear strength, as a measure of the interactions between the filler particle surface and the polymer molecules.[12,13] Some titanate and silane coupling agents have proved their efficacy in poly(propylene).[14–16] Davies[17] reported enhanced adhesion between PP and glass beads when the filler was surface-treated with aminosilanes. Nevertheless, although this kind of short molecules can promote a relatively strong bond with filler surface, through condensation reaction, they do not form either a chemical bond with poly(propylene) molecules or physical entanglements that can improve the cohesive strength of the material.[18] High molecular weight adhesion agents are preferred to promote physical entanglements with the matrix in the bulk. Poly(propylene) graft copolymers having polar comonomers are usually employed and have demonstrated efficacy.[19–23]

The use of some polar thermoplastic polymers, such as polyamide[24] or polycarbonate,[25] has been proposed as efficient adhesion promoters in filled PP composites. Following this idea, we analyze here the use of poly(ethylene terephthalate-*co*-isophthalate) (co-PET) in glass bead filled PP. The addition of co-PET into a poly(propylene) matrix has some drawbacks due to the poor compatibility between phases.[26–28] The noncompatibility can be overcome by adding into the blend compatibilizing agents. The addition of several types of PP graft copolymers, like those having maleic anhydride groups,[29–32] acrylic acid,[28] or glycidil methacrylate,[33] resulted in finely dispersed phases in the PP/co-PET blend, showing that these copolymers were able to compatibilize the blend. This compatibilizing efficiency has also been displayed by styrene-b-(ethylene-*co*-butylene)-b-styrene (SEBS) grafted with maleic anhydride groups (SEBS-g-MAH).[34,35] Lepers et al.[36] found that SEBS-g-MAH reduced the interfacial tension and prevented coalescence of the dispersed phase in PP/co-PET blends.

In the present article the microstructure and properties of PP/co-PET blends and their glass bead filled composites are shown, focused mainly on the effect of phase compatibilizing. Both untreated and silane-treated glass beads have been employed. The effect of co-PET, MAPP, and silane presence on the glass bead surface is analyzed.

MATERIALS, COMPOUNDING, AND SPECIMENS

The poly(propylene) was provided by Repsol-YPF (Puertollano, Spain). It was a homopolymer grade (Isplen PP050) with melt flow index (230°C, 2.16 kg) 5.0 dg/min. Glass beads with an average particle size of 20 μm were employed as filler, being provided by Sovitec Ibérica, S.A (Castellbisbal, Spain). Eastman Chemical (Madrid, Spain) supplied a commercial grade of maleated poly(propylene) (Epolene G-3003), with acid number 8. Extrupet EW36 was a copolymer grade of co-PET manufactured by Catalana de Polímers S.A. (El Prat de Llobregat, Spain), with intrinsic viscosity 0.8 dL/g.

PP/co-PET (95/5 wt.%) blends were prepared by melt extrusion. To improve the compatibilization MAPP was added, resulting in a PP/MAPP/co-PET blend (95/3/5 wt %). Also, PP/MAPP (97/3 wt %) and pure poly(propylene) were extruded in the same conditions for comparison.

Both untreated and silane treated glass beads were employed as filler (50 wt % in the composite). N-(2-(vinylbencylamino)-ethyl)-3-aminopropyl trimethoxy silane (Z-6032, Dow Corning, Seneffe, Belgium) was used as a coupling agent. The following procedure was used to homogeneously coat the glass bead with the silane: a solution containing 30 mL of silane, 250 mL of methanol, 60 mL of water, and 5 mL of acetic acid was prepared by 1.5 kg of glass beads. This solution was stirred for 20 min to assure silane alkoxy group hydrolysis. The solution was transferred into a flask, and glass beads were then added gradually while stirring. The mixture was then heated up to 40°C to evaporate the solvent. Stirring was continued as long as the viscosity of the mixture was low enough. The nonreacted silane was washed out with methanol.

Composites were prepared using a Collin ZK-35 twin screw extruder with 25 mm screw diameter and L/D ratio equal to 36. In composites containing co-PET, it was previously dried for a minimum of 4 h at 160°C and air of dew point −40°C. The extrusion temperature profile was from 150°C at the entrance to 250°C at the die, and the screw speed was fixed at 120 rpm. Vacuum devolatilizing was applied. A circular cross section die of 3-mm diameter was employed, and the extrudate was cooled in a water bath and pelletized.

Tensile dumbbell specimens (type "I" according to ASTM D638) were injection-molded using a Mateu and Solé 440/90 injection molding machine and a multi-propose mold (Fig. 4 of the ASTM D-647 standard) tempered at 60°C. To release residual stresses, the specimens were annealed at 110°C for 24 h.

TESTING

Wide-angle X ray diffraction (WAXD)

The experiments were performed using a Phillips PW 1050/71 diffractometer. Radial scans of intensity (I) versus scattering angle (2θ) were recorded in the range 5–50° at a scanning speed for the detector displace-

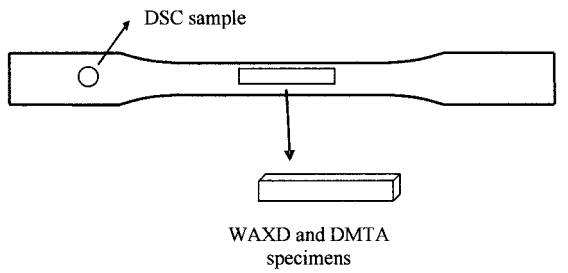

Figure 1 Injection-molded dumbbell specimen showing the sample extraction zone for DSC analysis and the machined prismatic specimen used in WAXD and DMTA analysis.

ment of 0.020/0.800 °/s by using filtered Cu K_a radiation. The testing was carried out using prismatic bars, extracted from the dumbbell specimens (Fig. 1), measuring nominally $25 \times 5 \times 3$ mm^3.

Vibrational spectroscopy

Compression-molded 0.2 mm-thick films were prepared with thee unfilled blends (PP, PP/co-PET, and PP/MAPP/co-PET) in a hot-plate press to be analyzed by Fourier transformed-infrared spectroscopy (FT-IR) and Raman. A Nicolet 510*M* and a Dilor XY Raman spectrometer were employed, respectively. The He/Ne laser (632.8 nm) of the Raman was polarized vertically, and the instrument operated exclusively in backscatter.

Differential scanning calorimetry (DSC)

DSC measurements were performed using a Perkin–Elmer Pyris 7 calorimeter. Calibration of the instrument was done using standard samples of In and Pb. The sample mass was typically 8–9 mg. It was extracted from the dumbbell specimens as shown in Figure 1. Once the sample thermal history was erased (4 min at 200°C), cooling cycles were conducted from 200 to 25°C applying different cooling rates: 5, 10, 15, 20, 25, 30, 40, and 60°C/min. All runs were carried out in a stream of dried nitrogen. After each cooling, a heating run between 25°C and 200°C was performed at 10°C/min. The crystallinity of PP was calculated according the following equation:

$$X_m = \frac{\Delta H_m (m_c/m_p)}{\Delta H_0} 100 \qquad (1)$$

where ΔH_m was the melting enthalpy measured in the heating experiments, ΔH_0 is the theoretical enthalpy of PP 100% crystalline ($\Delta H_0 = 207.1$ J/g)[37], m_c the mass of the sample, and m_p the mass of PP in the sample.

Differences in the PP nucleation rate were evaluated through the activity parameter (ϕ) obtained through the method developed by Dobreva and Gutzow.[38] The value of ϕ can decrease from 1 to 0 as the polymer nucleates in the presence of substrates. This approach has been successfully applied to evaluate nucleating rate differences of PP and other polymers filled with different mineral fillers and additives.[39–41]

Also, the following parameters were measured[42]: $T_c - T_p$ and Δw, T_p being the crystallization peak temperature and T_c the intercept of the base line with the tangent of the exotherm. This value gives information about the overall crystallization rate. Δw is the width at half height of the exotherm peak. As a general rule, a lower value of $T_c - T_p$ means faster overall crystallization rate, whereas a greater Δw value implies a broader crystalline size distribution.

Dynamic mechanical thermal analysis (DMTA)

DMTA testing was carried out using a Perkin–Elmer DMTA 7 machine, which was calibrated according to the standard procedure. The testing configuration was three-point bending with a support span of 20 mm. The samples employed were the same as for WAXD measurements. A static stress of 6 MPa and a dynamic stress of ± 5 MPa were applied with a frequency of 1 Hz.

For each specimen two kinds of tests were performed. On the one hand, dynamic loading was isothermally applied at 20°C to get quantitative results of the storage modulus (E′) and the loss tangent (tan δ). The values were taken 5 min after applying the stresses, that is, once the initial fluctuations of the values had disappeared. On the other hand, the study of the glass transition was carried out through tests performed in the range of temperature from −40 to 130°C, at a heating rate of 5°C/min.

Microscopy

A Zeiss polarizing optical microscope equipped with a Mettler hot stage was used to observe the PP spherulite nucleation and growth. The spherulite observation was carried out by utilizing sample sections 0.5 mm thick. The following procedure was used: the sample was heated at 200°C and kept at this temperature to destroy any traces of crystallinity, then the temperature was rapidly lowered to 137°C, and the sample was allowed to crystallize isothermally.

Information about the phase morphology of unfilled PP/co-PET and PP/MAPP/co-PET samples was performed through transmission electron microscopy (TEM). Microtomed sheets 200 nm thick were used. These cuts were stained[43] with RuO_4 and then observed on a JEOL 1200-EXII microscope.

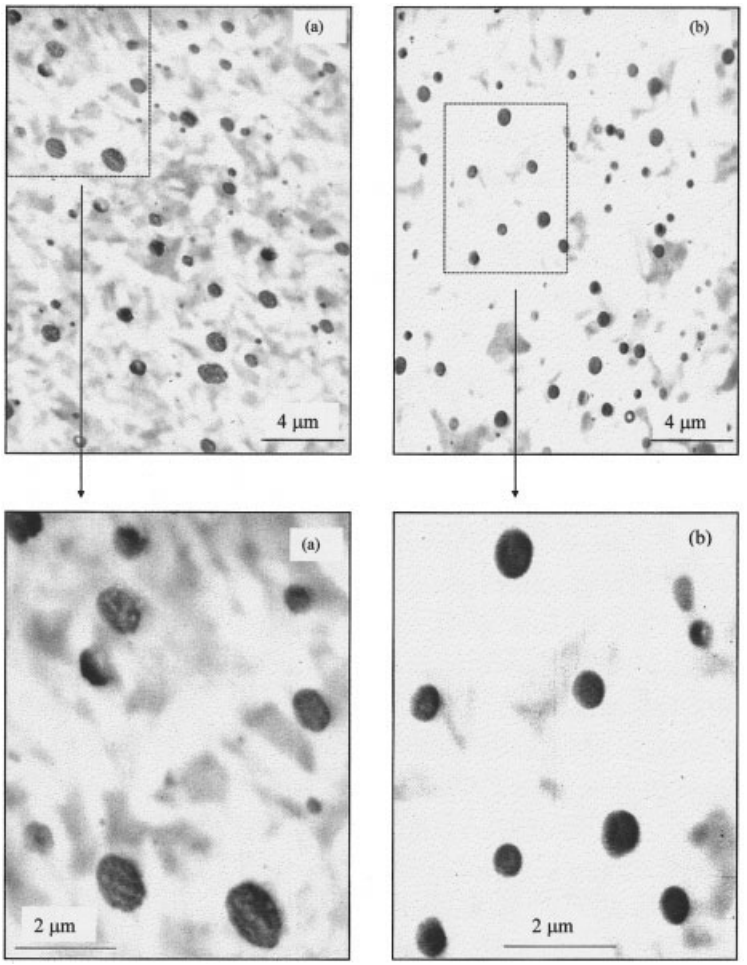

Figure 2 TEM micrographs of unfilled (a) PP/co-PET and (b) PP/MAPP/co-PET blends showing the phase dispersion and morphology of co-PET domains.

RESULTS AND DISCUSSION

Morphology of unfilled PP/co-PET blends

TEM micrographs of both PP/co-PET and PP/MAPP/co-PET blends displayed a two-phase pattern, with co-PET inclusions being approximately spherical in shape (Fig. 2). A reduction of the co-PET average domain size was noticed, along with a narrower size distribution, when MAPP was added (Fig. 3). This reduction could be related to the compatibilizing effect of MAPP in the PP/co-PET blend.[36] The average value of co-PET domains, as well as the size distribution curve, could be obtained from image analysis performed on the TEM pictures.

To support the former observation, a comparison of FT-IR spectra of PP/co-PET and PP/MAPP/co-PET blends was carried out after subtracting the pure PP spectrum (Fig. 4). An increase in the intensity of the CH_2 and CH_3 deformation bands in the 1480–1360 cm^{-1} range was observed in the compatibilized PP/MAPP/co-PET blend. Furthermore, it could be noticed that the band at 1345 cm^{-1} (CH_2 wag), related to

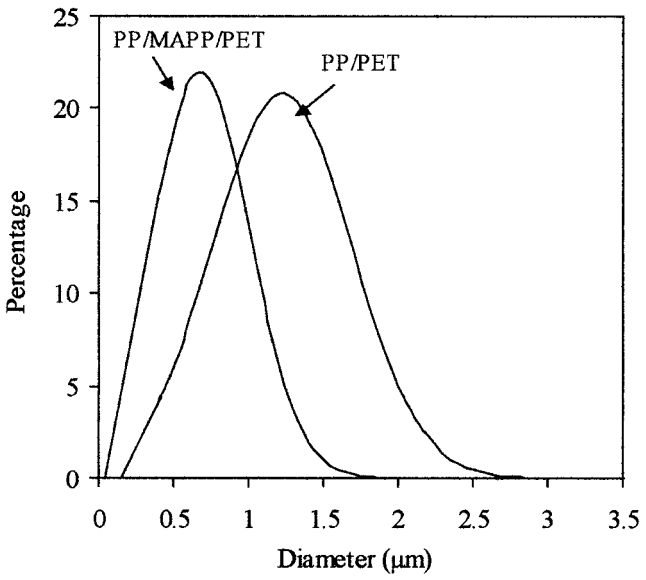

Figure 3 Average size distribution of co-PET inclusions for unfilled PP/co-PET and PP/MAPP/co-PET blends.

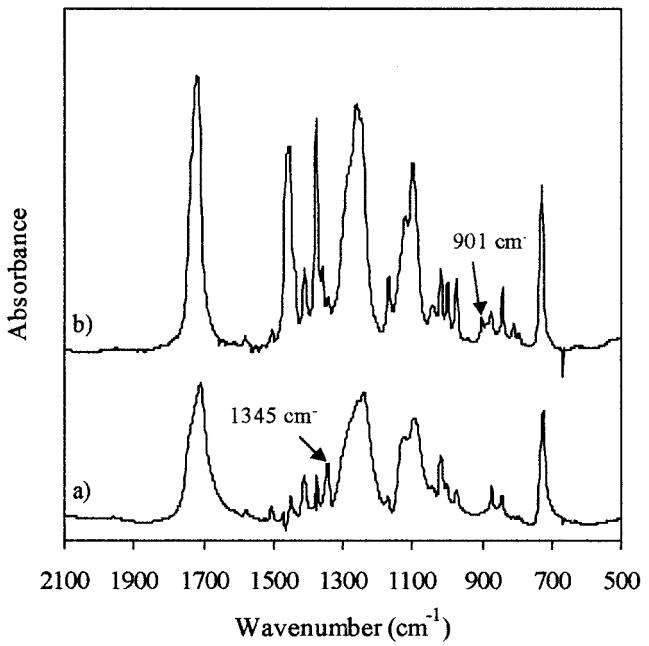

Figure 4 FT-IR spectra of unfilled (a) PP/co-PET and (b) PP/MAPP/co-PET blends after subtracting the neat PP spectra.

the crystalline co-PET structure,[44] was more intense in sample PP/co-PET than in PP/MAPP/co-PET blend. As well, the band at 901 cm^{-1} (CH_2 rock gauche configuration), related to the co-PET amorphous phase, appeared in the presence of MAPP. According to this, MAPP has proved to be effective as a compatibilizing agent for PP and co-PET, causing the reduction of both size and crystallinity of co-PET domains in the blend.

By Raman, the compatibilizing effect of MAPP for the PP/co-PET blend could also be observed. Changes in both 973 cm^{-1}/997 cm^{-1} and 1151 cm^{-1}/1167 cm^{-1} intensity ratios have been related[45] to changes in PP molecular orientation and crystallinity. As can be seen in Figure 5, no differences in these intensity ratios can be observed for PP/co-PET blend with regard to pure PP, but can be observed in the PP/MAPP/co-PET blend.

Crystallization behavior

Characteristics obtained from DSC are summarized in Table I. Examples of crystallization exotherm patterns and plots of Dobreva and Gutzow analysis are shown in Figures 6 and 7, respectively. Focusing on unfilled samples, it can be observed that the addition of co-PET increased dramatically the value of the crystallization peak temperature of PP cooled from the melt. A remarkable increase of the PP crystallization temperature has been reported[46] in composites of poly(propylene) with co-PET fibers. In these composites, co-PET fibers induced transcrystallinity. In our case, transcrystallinity could not be observed as the co-PET phase appears as small dispersed droplets.

The nucleation activity parameter (ϕ) fell to 0.52 when co-PET was added to PP (sample PP/co-PET), indicating a high nucleating rate. Moreover, a faster overall crystallization rate could be deduced from a lower $T_c - T_p$ value in this sample. Both effects would lead to a narrower crystalline size distribution, as a lower value of Δw indicates.[42]

MAPP addition in both the PP and PP/co-PET blend did not modify PP crystallization characteristics. Some researchers[47–49] have reported that small amounts of MAPP act as nucleating agents in homopolymer PP, although we have not observed this effect.

It is generally accepted that a faster nucleating rate can be related with smaller crystalline sizes in poly(propylene).[50] Figure 8 illustrates the effect of co-PET presence on the crystalline size of PP. From microscope analysis carried out on samples after isothermal crystallization, a reduction of the spherulite mean size, from approximately 25 μm to 15 μm, could be observed in PP when co-PET was added. No effect was noticed due to MAPP.

In glass filled samples, a remarkable increase in the nucleation rate was evidenced by both a build-up in the T_p and a reduction in ϕ values. Nevertheless, these effects due to glass beads were less marked than that of co-PET. In this sense, the nucleating efficiency of both glass spheres[1] and glass fibers[51] into PP has been

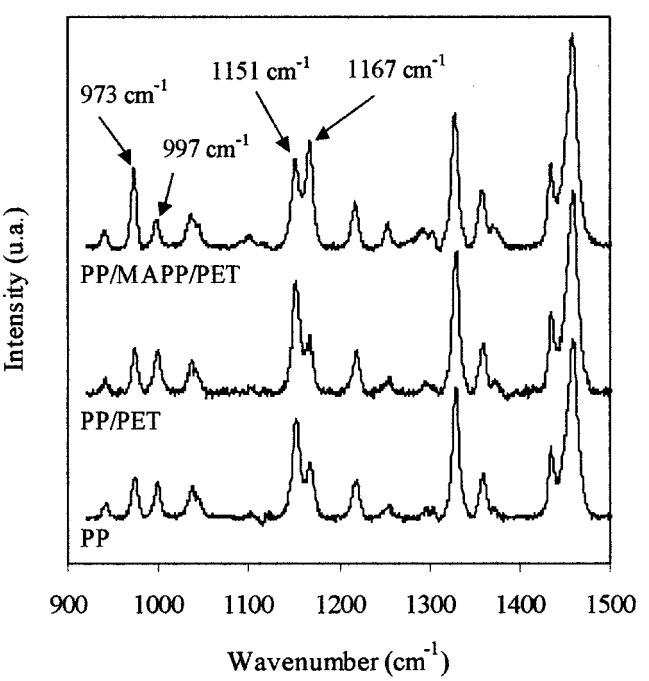

Figure 5 Raman spectra of unfilled (a) PP/co-PET and (b) PP/MAPP/co-PET blends.

TABLE I
Crystallization and Melting Characteristics Obtained from DSC

Samples		Crystallization					Melting	
		T_c (°C)	T_p (°C)	$T_c - T_p$	Δw	ϕ	T_m (°C)	X_m (%)
Unfilled polymer blends	PP (1)	118.8	113.9	4.9	4.8	1.00	163.7	55.5
	PP/MAPP (2)	120.3	115.3	5.0	5.0	1.00	160.1	53.8
	PP/co-PET (3)	129.2	125.6	3.6	4.5	0.52	165.7	57.3
	PP/MAPP/co-PET (4)	129.3	125.1	4.2	4.7	0.51	164.6	56.2
Untreated (U) glass bead composites	U1	123.7	120.9	2.8	3.2	0.72	162.5	53.9
	U2	128.1	123.5	4.6	4.4	0.53	164.7	56.8
	U3	129.2	126.5	2.7	3.1	0.49	164.4	60.5
	U4	129.6	127.5	2.1	2.5	0.52	164.4	61.3
Silane-treated (T) glass bead composites	T1	125.5	122.6	2.9	3.1	0.66	163.4	56.0
	T2	127.5	124.2	3.3	3.5	0.55	163.1	52.5
	T3	129.0	126.5	2.5	2.9	0.49	164.1	59.3
	T4	131.2	128.2	3.0	3.2	0.41	165.1	58.2

reported. The nucleating activity of glass beads into PP is less effective than that displayed by mineral fillers like talc[39] ($\phi = 0.32$), magnesium hydroxide[40] ($\phi = 0.52$), or aluminum hydroxide[41] ($\phi = 0.54$). Furthermore, a slight reduction of Δw was found in glass bead filled PP, as a consequence of a slightly faster overall crystallization rate ($T_c - T_p$).

MAPP presence enhanced the nucleation activity of glass beads, leading to a significant reduction in ϕ values for all the composites with PP/MAPP matrix. This higher nucleation rate did not imply a greater overall crystallization rate, as no remarkable differences were found in the values of the parameter $T_c - T_p$, with respect to that showed by neat PP. Moreover, no variations were found in the crystalline size distribution. These results suggested a lower crystalline growth in these composites.

On the other hand, glass bead addition into PP/co-PET and PP/MAPP/co-PET blends did not lead to a remarkable difference in the values of ϕ when compared with unfilled blends. Nevertheless, a greater overall crystallization rate, which resulted in narrower crystalline size distribution (lower Δw values), was noticed. It should be pointed out that in filled samples it was not possible to analyze the crystalline texture of poly(propylene) through optical microscopy due to the high amount of filler incorporated.

With respect to the surface treatments applied onto glass beads, although controversial opinions are found in the literature, in this work it was noticed that

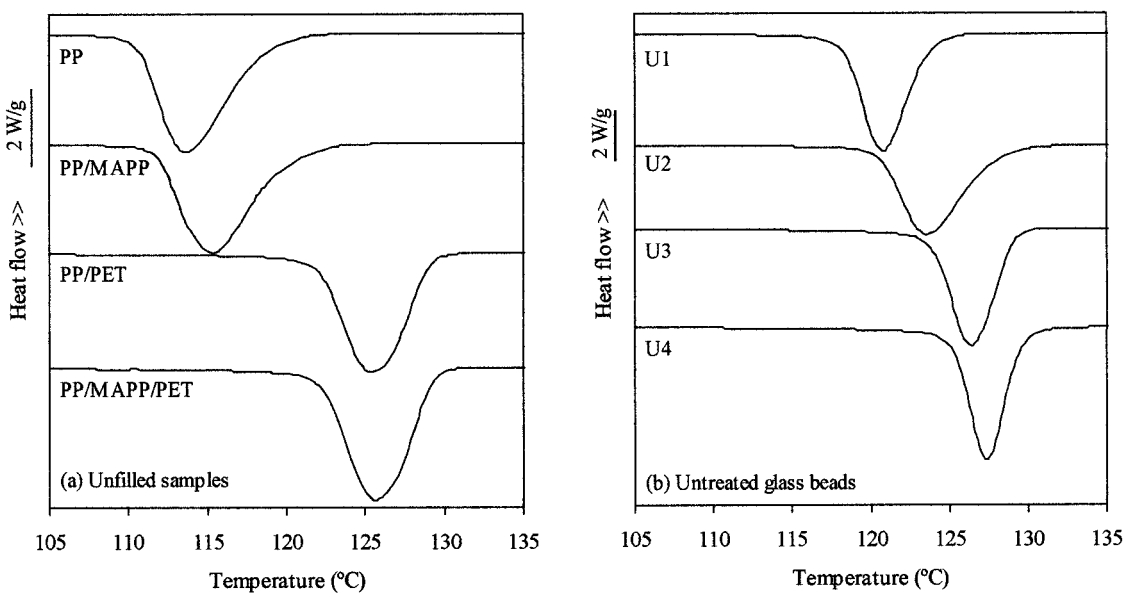

Figure 6 DSC crystallization patterns of (a) unfilled blends and (b) composites with untreated glass beads. Cooling rate 10°C/min.

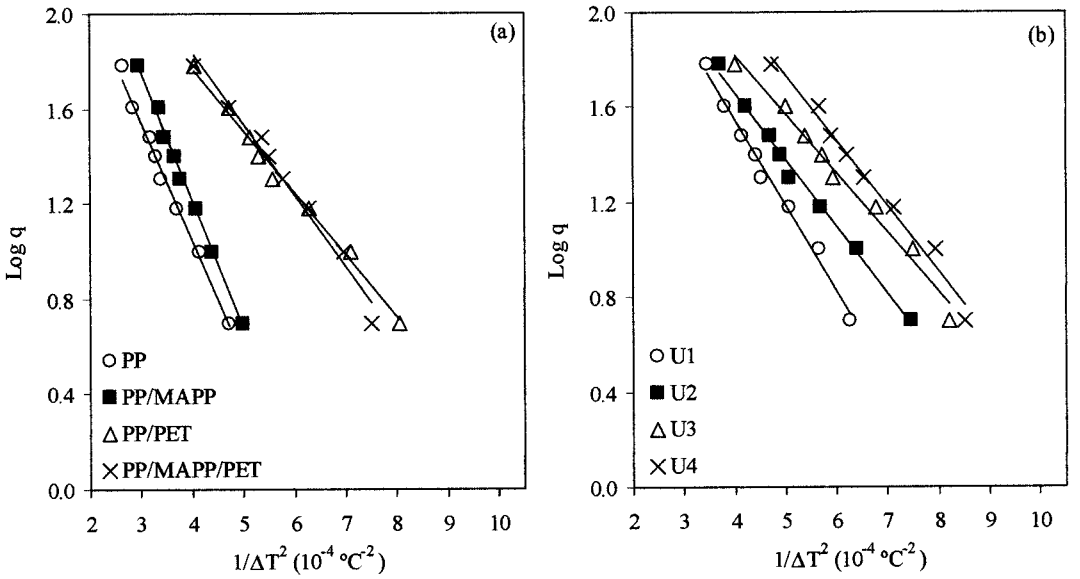

Figure 7 Linear fits of the cooling rate (q) versus the supercooling (ΔT) values for (a) unfilled blends and (b) untreated glass bead composites.

the use of the silane Z-6032 enhanced slightly the nucleation activity of glass beads.

Focusing on the melting behavior, an asymmetrical and wide signal of neat poly(propylene), usually related to a progressive melting of crystalline entities, can be seen (Fig. 9a). The addition of MAPP resulted in a drop of the melting peak temperature (Table I), probably because grafted maleic anhydride hinders the molecular rearrangement of PP and thus forms less perfect crystals.

The presence of co-PET in both PP and PP/MAPP compositions led to an increase in the melting peak temperature, accompanied with a narrower signal, which would be due to the nucleating effect of co-PET, which results in a finer crystalline texture of PP, usually related to the higher melting peak temperature.

On the other hand, the addition of glass beads produced significant differences when a PP/MAPP matrix was employed (Fig. 9b), as the T_m values increased notably with respect to the unfilled PP/MAPP blend, while in composites with co-PET presence no remarkable variations were noticed.

A considerable reduction in the supercooling degree ($T_m - T_p$) is observed, when comparing both unfilled

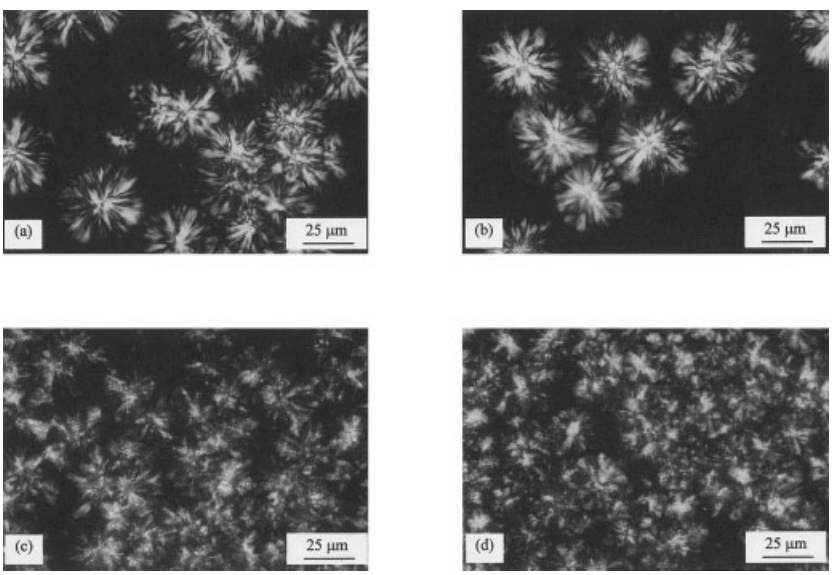

Figure 8 Cross polarized optical pictures of unfilled blends after isothermal crystallization for (a) PP, (b) PP/MAPP, (c) PP/co-PET, and (d) PP/MAPP/co-PET.

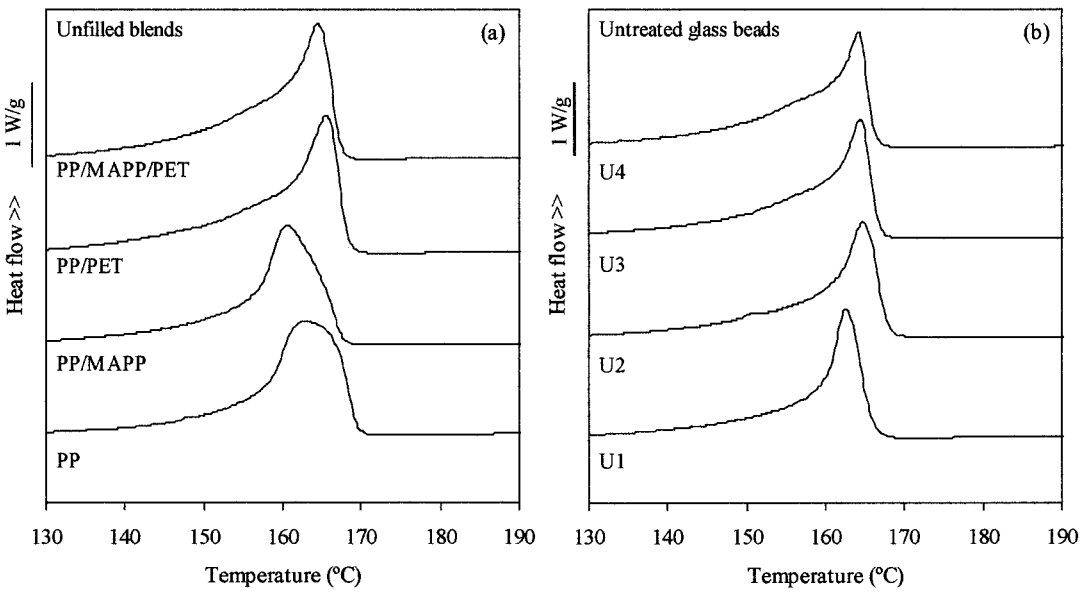

Figure 9 DSC melting endotherms after cooling at 10°C/min of (a) unfilled blends and (b) composites with untreated glass beads.

blends and composites with pure PP. This decrease in the supercooling degree is a typical feature of polymers filled with particles able to nucleate, and thus, the small increase in the melting temperature values cannot be attached to a higher stability of the crystalline entities, but kinetic differences.

Small differences have been found in the crystallinity values (Table I), which can be taken as a result of experimental error.

Orientation of the crystalline phase

The orientation of monoclinic α-phase PP crystals in the injection-molded samples has also been studied by WAXD. The diffraction patterns and main Miller indexes of some characteristic materials are shown in Figure 10. The relationship between the orientation of PP a- and b-axes can be determined by taking the ratio of the intensity of the PP (040) plane (peak at $2\theta = 16.7°$ in the diffraction pattern) to the (110) plane (peak at $2\theta = 13.9°$), and the results are summarized in Table II. The higher ratio value, the higher the orientation. Several values of this ratio are found in the literature for filled poly(propylene),[40,52] and some authors have even given a value for an isotropic mixture of PP crystallites, that is, 0.54,[53] and values comprised between 0.67 and 0.77.[54]

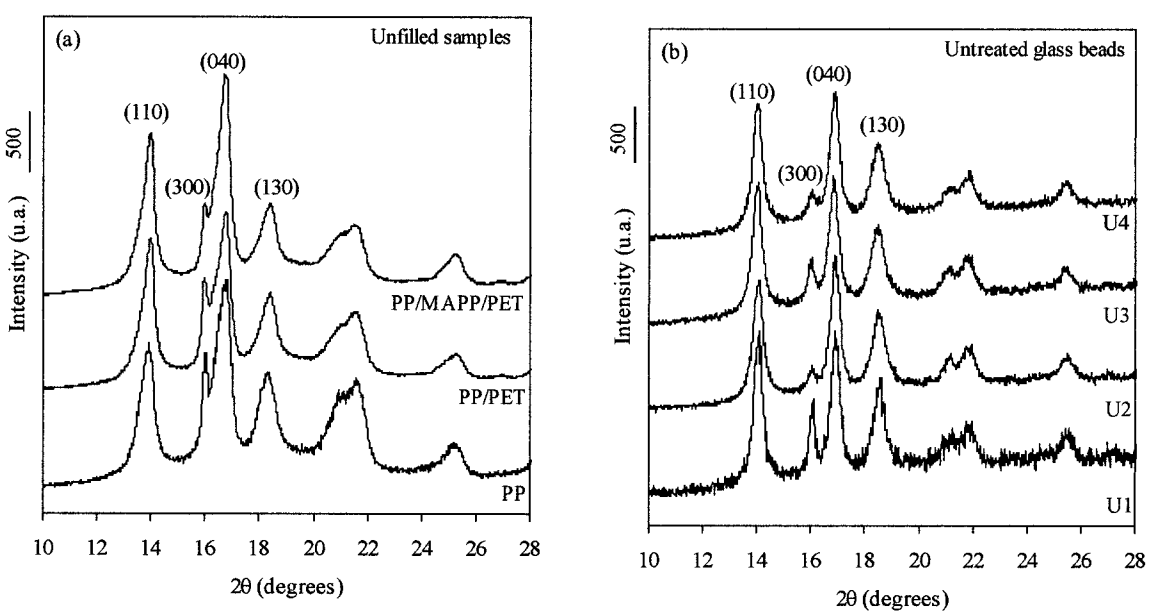

Figure 10 Wide angle X-ray scattering patterns of (a) unfilled blends and (b) composites with untreated glass beads.

TABLE II
Values of Poly(propylene) Crystallinity (X_{WAXD}), b-Axis Orientation, I(040)/I(110), and β Phase Fraction ($\beta/\alpha + \beta$)

Samples		X_{WAXD} (%)	$\frac{I(040)}{I(110)}$	$\frac{\beta}{\alpha + \beta}$
Unfilled polymer blends	PP (1)	42.4	1.44	0.17
	PP/MAPP (2)	—	—	—
	PP/co-PET (3)	45.9	1.17	0.21
	PP/MAPP/co-PET (4)	45.4	1.35	0.17
Untreated (U) glass bead composites	U1	49.9	0.98	0.15
	U2	52.3	1.17	0.11
	U3	50.8	1.05	0.15
	U4	49.9	1.08	0.13
Silane-treated (T) glass bead composites	T1	49.9	0.90	0.17
	T2	48.3	1.07	0.11
	T3	49.0	0.93	0.15
	T4	51.9	1.02	0.13

Both co-PET and glass bead addition into PP led to intensity ratios close to 1, resulting in an homogenization of the poly(propylene) orientation. The co-PET effect contrasts with that observed by Saujanya[55] in PET fiber-reinforced PP composites, since the crystallite growth along the b-axis is notably affected by the presence of PET fibers, increasing the orientation of the poly(propylene) b-axis. It should be noted that substrates with high aspect ratios usually involve transcrystallinity structures in poly(propylene),[56,57] allowing a preferential location of poly(propylene) chains. Glass beads do not promote this effect. The high amount of glass beads incorporated would be a possible reason of the hindered preferential orientation of poly(propylene) chains during the mold filling.[58]

On the contrary, MAPP promoted PP orientation. The compatibilizing effect of this copolymer involved PP rearrangements that could affect the orientation of the PP crystal.

It is possible to give an estimation of the crystallinity from X-ray diffraction patterns, from the ratio between the crystalline phase signal and the total signal, applying the methodology of Weidinger and Hermans.[59] Nevertheless, due both to the determination of the baseline and the interference of various signals, the obtained crystallinity has to be taken as a relative value. For unfilled blends, the crystallinity followed a similar trend as observed in DSC experiences, as crystallinity slightly increases with co-PET presence. All the filled composites showed crystallinity values between 48 and 51%, slightly higher than that of neat PP.

WAXD measurements also provided information about the presence of the β-phase. As shown in Figure 10, this crystalline phase, plane (300) appears at $2\theta = 16.7$. The main factors involved in the nucleation and crystallization of the β-phase in PP have been studied by Varga.[50] It has been established that this kind of crystallization appears for crystallization temperatures below approximately 140°C. For filled polymers in which the filler acts as a nucleating agent and at temperatures above the previous critical value, the polymer mainly crystallizes in the α-modification. In addition, high shear stresses promote PP β-phase formation. It should be also mentioned that WAXD measurements have been performed in the sample surface close to the mold surface, where both shear stress and cooling rate into the mold are much higher, which enhances the β-phase formation.

It is possible to give an estimation of the β-phase fraction through the parameter proposed by Turner–Jones.[60] The presence of co-PET increased the percentage of β-phase, whereas MAPP reduced it in the glass bead containing samples.

Dynamical-mechanical thermal behavior

Storage modulus values obtained from isothermal tests (Table III) showed in unfilled samples that the addition of co-PET led to a slight build-up of the stiffness. This increase is higher when MAPP is added, probably due to the compatibilizing effect of MAPP in the PP/co-PET blend. The presence of glass beads in the PP matrix increases dramatically the stiffness of the compound.

A decrease (Table III) was observed in the value of the loss tangent in adding co-PET to the poly(propylene) matrix, in consonance with the work of López-Manchado et al. on co-PET-fiber reinforced PP composites.[61] This is due to the slight increase appreciated in the storage modulus value. Moreover, at room temperature, co-PET is under its glass transition temperature, and thus the viscous dissipation phenomena of the blend are reduced. A further reduction of the loss tangent value is observed in the blend PP/MAPP/co-PET. This fact has been related to an enhanced interfacial adhesion between phases,[22] which hinders the molecular motion of poly(propylene) chains close to the interface, and thus the viscous dissipation phenomena are constrained.

TABLE III
Storage Modulus and Loss Factor Values from the Isothermal DMTA Analysis, and Glass Transition and α′ Relaxation Temperatures from the Non-isothermal DMTA Analysis

Samples		E′ (GPa)	tan δ	T_g (°C)	$T_{\alpha'}$ (°C)
Unfilled polymer blends	PP (1)	1.6	0.054	−0.80	52.37
	PP/MAPP (2)	—	—	—	—
	PP/co-PET (3)	1.7	0.046	0.34	52.14
	PP/MAPP/co-PET (4)	1.9	0.042	0.75	54.62
Untreated (U) glass bead composites	U1	3.0	0.041	−1.07	56.06
	U2	2.8	0.040	0.20	57.65
	U3	3.1	0.034	0.06	57.07
	U4	3.4	0.032	0.63	64.52
Silane-treated (T) glass bead composites	T1	3.2	0.030	0.61	59.44
	T2	3.0	0.032	0.85	61.71
	T3	3.3	0.029	1.19	61.88
	T4	3.4	0.031	1.34	59.22

A remarkable diminution of the tan δ value when filling PP with 50% of untreated glass beads occurs. As commented previously, the values of the storage modulus increases markedly when adding glass beads and thus the tan δ values are reduced. Surface treatment of the glass beads leads to a further slight reduction.

Loss modulus (E″) of neat PP as well as glass bead filled samples have maximums around 0°C (Fig. 11), corresponding with the glass transition temperature of poly(propylene) (T_g). The obtained values for the glass transition temperature are collected in Table III. Small differences have been found, as the values ranged between −1 and 1°C. Nevertheless, as a general trend, it was observed that composites containing MAPP showed higher T_g values than is homologous without this copolymer. Also, the highest values for each matrix composition were displayed by the samples with glass beads treated with silane Z-6032. This slight build-up could be related with a higher[62] interaction degree between matrix and filler.

Both unfilled and filled samples displayed an additional maximum ($T_{\alpha'}$) located around 50–70°C (Fig. 11). Focusing on unfilled samples, it was found that both the temperature and the intensity of this relaxation was very similar for pure PP and PP/co-PET blend, while in the PP/MAPP/co-PET blend the $T_{\alpha'}$ value shifted to higher temperatures and the intensity of the signal was stronger (Fig. 11a).

The addition of glass beads into PP gave a stronger signal (Fig. 11b) than that of pure PP and also appears

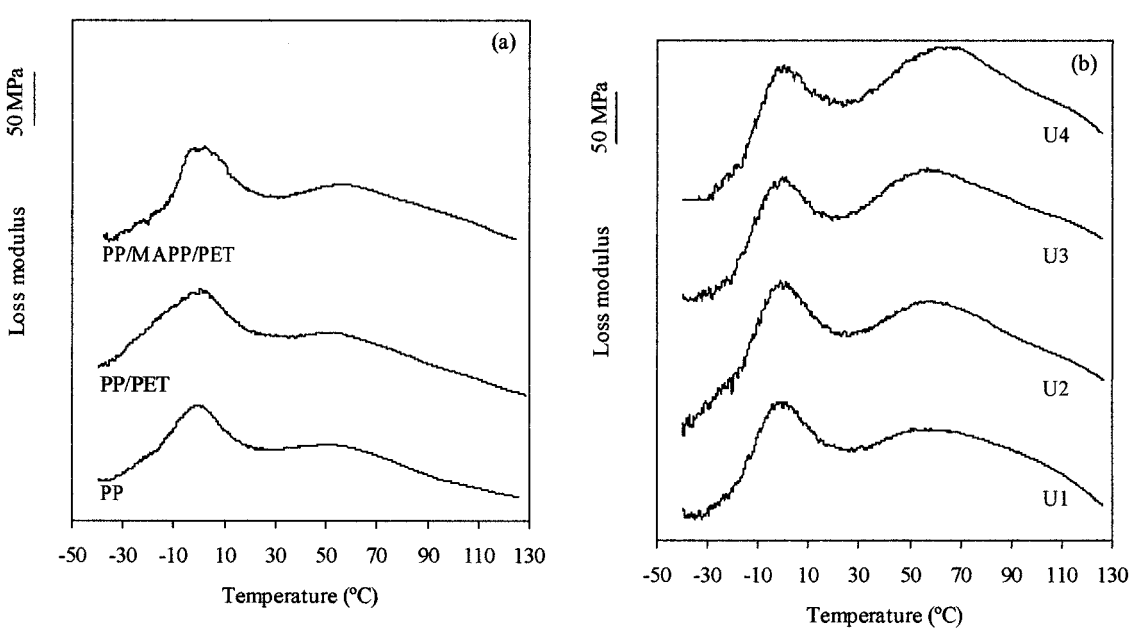

Figure 11 Loss modulus (E″) versus temperature DMTA plots of (a) unfilled blends and (b) composites with untreated glass beads.

at higher temperatures. It was also noticed that in glass bead-filled PP/co-PET and PP/MAPP/co-PET composites, the intensity of the relaxation was stronger than those of the composites without co-PET. Glass bead surface treatment seemed to increase in most cases the values of $T_{\alpha'}$.

Controversial opinions are found in the literature about this transition shown by PP. McCrum ascribes this relaxation to both mechanisms of lamellar slipping and rotation between crystalline entities.[63] Jančář[62] supposes that this maximum is the consequence of a release of strongly hindered segmental mobility of molecules from the interface on the filler surface is probably the glass transition peak of PP immobilized on the filler surface. However, he reported the appearance of this relaxation with filler contents above 26% vol. and it was not seen in unfilled PP. On the other hand, Stricker et al.[2] attribute the appearance of these transitions to the quenching effect in the melts of PP filled with glass bead, noticing that slow cooling and crystallization avoid this effect.

The values of the maximum of the α' relaxation ($T_{\alpha'}$) are collected in Table III, and on the contrary, as observed by Jančář, in the unfilled samples we have observed the appearance of this relaxation. Both the intensity and temperature were found to be similar for poly(propylene) as for PP/co-PET blend (Fig. 11a). On the other hand, in the blend PP/MAPP/co-PET, the relaxation is more intense and shifted to higher temperatures, which might be a consequence of the compatibilizing effect exerted by MAPP.

In the filled composites, the relaxation α' showed the highest intensities; also, co-PET presence provokes a build-up of the intensity. Also, it is noticeable that silane surface treatment increased the value of $T_{\alpha'}$ with respect to those showed by composites with untreated glass beads.

From the obtained results, it appears that this relaxation α' depends on the interactions between PP and the other phases (glass bead and co-PET), increasing its intensity and shifting to higher temperatures when both glass and co-PET are added, as well as with the addition of MAPP and the glass bead surface treatment. Nevertheless, the appearance of this relaxation in the unfilled PP involves a relationship with the PP crystallinity, and may suggest that the special molding conditions (mold temperature 60°C, cooling time 30 s, annealing at 110°C for 24 h) applied on the PP could have induced a particular crystalline structure that is able to progress to more stable states under the DMTA testing conditions. This evolution would consist, according to McCrum and Jančář, in a reorganization of lamellar blocks.

A further DMTA analysis under isothermal conditions could reveal a possible temporal evolution of this relaxation, which would help to clarify the influence of the thermal story on the relaxation α'.

CONCLUSION

The effect of filling PP with glass beads and/or co-PET has been studied. The morphology of the blend PP/co-PET was influenced by the presence of MAPP because of its compatibilization action. The co-PET domains were found to be smaller, less crystalline, and with smoother boundaries than those found in the blend without MAPP. Changes in FT-IR and Raman spectra supported the compatibilization evidence.

Co-PET presence promoted faster PP crystallinity nucleation, and reduction of the crystalline sizes was noticed, giving place to improved dynamic-mechanical properties.

The orientation of PP α-crystals was studied by WAXD. A slight reduction in PP b-axis orientation could be determined in the filled samples with respect to unfilled PP. No remarkable effects concerning the silane coupling agent were observed.

The PP storage modulus increased slightly with the addition of co-PET, and dramatically when glass beads were added, whereas the loss tangent followed the opposite tendency. In addition, the loss tangent also decreased when the silane treatment was used. Slight increments in the PP glass transition temperature were noticed due to co-PET presence and/or silane coupling agent on the glass surface. Under the applied molding conditions the PP α' relaxation appeared in the interval 50–70°C, which could be related with a structural evolution of the polymer to more stable states.

The authors gratefully acknowledge financial support from the MCYT (Government of Spain) (MAT-2000–1112, MAT-2000–0084-P4, and DPI-2000–0184-P4 projects). Also, D. Arencón thanks the CIRIT (Government of Catalonia, Spain) for the concession of a Ph.D. grant.

References

1. Stricker, F.; Bruch, M.; Mülhaupt, R. Polymer 1997, 38, 5347.
2. Stricker, F.; Maier, R. D.; Bruch, M.; Thomann, R.; Mülhaupt, R. Polymer 1999, 40, 2077.
3. Liang, J. Z.; Li, R. K. Y. Polym Int 2000, 49, 170.
4. Liang, J. Z.; Li, R. K. Y.; Tjong, S. C. Polym Testing 2000, 19, 213.
5. Faulkner, D. L.; Schmidt, L. R. Polym Engng Sci 1997, 17, 657.
6. Schmidt, L. R. Polym Engng Sci 1997, 17, 666.
7. Liang, J. Z.; Li, R. K. Y. Polym Compos 1998, 19, 698.
8. Sjöngren, B. A.; Berglund, L. A. Polym Compos 1997, 18, 1.
9. Liang, J. Z.; Li, R. K. Y. J Reinforc Plast Compos 2001, 20, 630.
10. Liang, J. Z.; Li, R. K. Y. Polymer 1999, 40, 3191.
11. Asp, L. E.; Sjöngren, B. A.; Berglund, L. A. Polym Compos 1997, 18, 9.
12. Ishida, H. Interfaces in Polymer, Ceramic and Metal Matrix Composites; Elsevier: New York, 1988.
13. Pukánszky, B. Composites 1990, 21, 255.
14. Plueddemann, E. P. Silane Coupling Agents; Plenum Press: New York, 1982.
15. Bajaj, P.; Jha, N. K.; Jha, R. K. Polym Engng Sci 1989, 29, 557.
16. Witucki, G. L. J Coating Technology 1993, 65, 57.

17. Davies, L. C.; Sothern, G. R.; Hodd, K. A. Plast Rubber Process Appl 1985, 5, 9.
18. Jančář, J. J Mater Sci 1989, 24, 4268.
19. Stamhuis, J. E. Polym Compos 1988, 9, 72.
20. Xavier, S. F.; Schultz, J. M.; Friedrich, K. J Mater Sci 1990, 25, 2411.
21. Felix, J. M.; Gatenholm, P. J Appl Polym Sci 1991, 50, 699.
22. Bikiaris, D.; Matzinos, P.; Larena, A.; Flaris, V.; Panayiotou, C. J. J Appl Polym Sci 2001, 81, 701.
23. García-Martínez, J. M.; Laguna, O.; Areso, S.; Collar, E. P. J Appl Polym Sci 2001, 81, 625.
24. Ulrich, M.; Caze, C.; Laroche, P. J Appl Polym Sci 1998, 67, 201.
25. Noh, C. H.; Yoon, B. S.; Suh, M. H.; Lee, S. H. Polymer 2001, 42, 2695.
26. Rudin, A.; Loucks, D. A.; Goldwasser, J. M. Polym Engng Sci 1980, 20, 741.
27. Bataille, P.; Boissé, S.; Schreiber, H. P. Polym Engng Sci 1987, 27, 622.
28. Xanthos, M. Polym Engng Sci 1988, 28, 1392.
29. Xanthos, M.; Young, M. W.; Biesenberger, J. A. Polym Engng Sci 1990, 30, 355.
30. Cheung, M. K.; Chan, D. Polym International 1997, 43, 281.
31. Yoon, K. H.; Lee, H. W.; Park, O. O. J Appl Polym Sci 1998, 70, 389.
32. Pang, Y. X.; Jia, D. M.; Hu, H. J.; Hourston, D. J.; Song, M. Polymer 2000, 41, 357.
33. Champagne, M. F.; Huneault, M. A.; Roux, C.; Peyrel, W. Polym Engng Sci 1999, 38, 976.
34. Heino, M.; Kirjava, J.; Hietaoja, P.; Seppälä, J. J Appl Polym Sci 1997, 65, 241.
35. Papadopoulou, C. P.; Kalfoglou, N. K. Polymer 2000, 41, 2543.
36. Lepers, J. C.; Favis, B. D.; Tabar, R. J. J Polym Sci Part B: Polym Phys 1997, 35, 2271.
37. Wunderlich, B. Thermal Analysis; Academic Press: New York, 1990.
38. Dobreva-Veleva, A.; Gutzow, I. J Non Cryst Solids 1993, 162, 13.
39. Alonso, M.; Velasco, J. I.; de Saja, J. A. Eur Polym Mater 1997, 33, 255.
40. Velasco, J. I.; Morhain, C.; Martínez, A. B.; Rodríguez-Pérez, M.A.; de Saja, J. A. Macromol Mater Eng 2001, 286, 719.
41. Velasco, J. I.; Morhain, C.; Martínez, A. B.; Rodríguez-Pérez, M.A.; de Saja, J. A. Polymer 2002, 43, 6813.
42. Maiti, S. N.; Mahapatro, P. K. Int J Polym Mater 1990, 14, 205.
43. Trent, J. S.; Scheinbeim, J. I.; Couchman, P. R. Macromolecules 1983, 16, 589.
44. Noda, I.; Dowrey, A. E.; Marcott, C. Physical Properties of Polymers Handbook; American Institute of Physics: Woodbury, NY, 1996.
45. Fraser, G. V.; Hendra, P. J.; Watson, D. S.; Gall, M. J.; Willis, H. A.; Cudby, M. E. A. Spectrochimica Acta 1973, 29A, 1525.
46. López Manchado, M. A.; Arroyo, M. Polymer 1999, 40, 487.
47. Duvall, J.; Sellitti, C.; Myers, C.; Hiltner, A.; Baer, E. J. J Appl Polym Sci 1994, 52, 207.
48. Cho, K.; Li, F.; Choi, J. Polymer 1999, 40, 1719.
49. Seo, Y.; Kim, J.; Kim, K. U.; Kim, Y. C. Polymer 2000, 41, 2639.
50. Varga, J. J Mater Sci 1992, 27, 2557.
51. Bogoeva-Gaceva, G.; Janevski, A.; Mader, E. Polymer 2001, 42, 4409.
52. Díez-Gutiérrez, S.; Rodríguez-Pérez, M. A.; de Saja, J. A.; Velasco, J. I. Polymer 1999, 40, 5345.
53. Addink, E. J.; Beintema, J. Polymer 1961, 2, 185.
54. Rybnikar, F. J Appl Polym Sci 1989, 38, 1479.
55. Saujanya, C.; Radhakrishnan, S. Polymer 2001, 42, 4537.
56. Tan, J. K.; Kitano, T.; Hatakeyama, T. J Mater Sci 1990, 25, 3380.
57. Thomason, J. L.; Van Rooyen, A. A. J Mater Sci 1992, 27, 889.
58. Gordillo, A. Ph.D. Thesis, Universitat Politècnica de Catalunya, Barcelona, 2000.
59. Alexander, L. E. X-Ray Diffraction Methods in Polymer Science; Wiley-Interscience: New York, 1969.
60. Turner-Jones, A.; Aizlewood, J. M.; Beckett, D. R. Makromol Chem 1964, 75, 134.
61. López-Manchado, M. A.; Arroyo, M. Polymer 2001, 41, 7761.
62. Jančář, J. J Mater Sci 1991, 26, 4123.
63. McCrum, E.; Read, B. E.; Williams, G. Anelastic and Dielectric Effects in Polymeric Solids; Wiley: London, 1967.